



Supplement of

Anthropogenic CO₂ emission estimates in the Tokyo metropolitan area from ground-based CO₂ column observations

Hirofumi Ohyama et al.

Correspondence to: Hirofumi Ohyama (oyama.hirofumi@nies.go.jp) and Matthias M. Frey (frey.matthias.max@nies.go.jp)

The copyright of individual parts of the supplement might differ from the article licence.

Supplementary material

Table S1. Biogenic CO₂ fluxes used for estimating the XCO₂ uncertainty resulting from the uncertainty in the biogenic flux.

Data	Temporal resolution	Spatial resolution	Flux
VISITc*	Hourly	~0.31°	Net ecosystem exchange
SiB4	Hourly	0.5°	Net ecosystem exchange
CarbonTracker 2019B	3-hourly	1°	Optimized biogenic and oceanic fluxes
BEAMS	Monthly	30 arcsec	Net ecosystem exchange

*Downscaled by green vegetation fraction data

Table S2. Annual CO₂ emissions in fiscal year 2015 reported by four administrative divisions located in southern Kanto.

Division	Annual CO ₂ emission (Mt-CO ₂ yr ⁻¹)	Reference
Tokyo	60.33	https://www.kankyo.metro.tokyo.lg.jp/en/climate/index.files/Tokyo_GHG_2019.pdf
Chiba	78.497	https://www.pref.chiba.lg.jp/shigen/chikyuukankyou/documents/2017haisyutsuryou.pdf
Kanagawa	70.24	https://www.pref.kanagawa.jp/documents/9881/g hg_siryō.pdf
Saitama	41.541	https://www.pref.saitama.lg.jp/documents/25672/r4zentaihoukokusyo.pdf

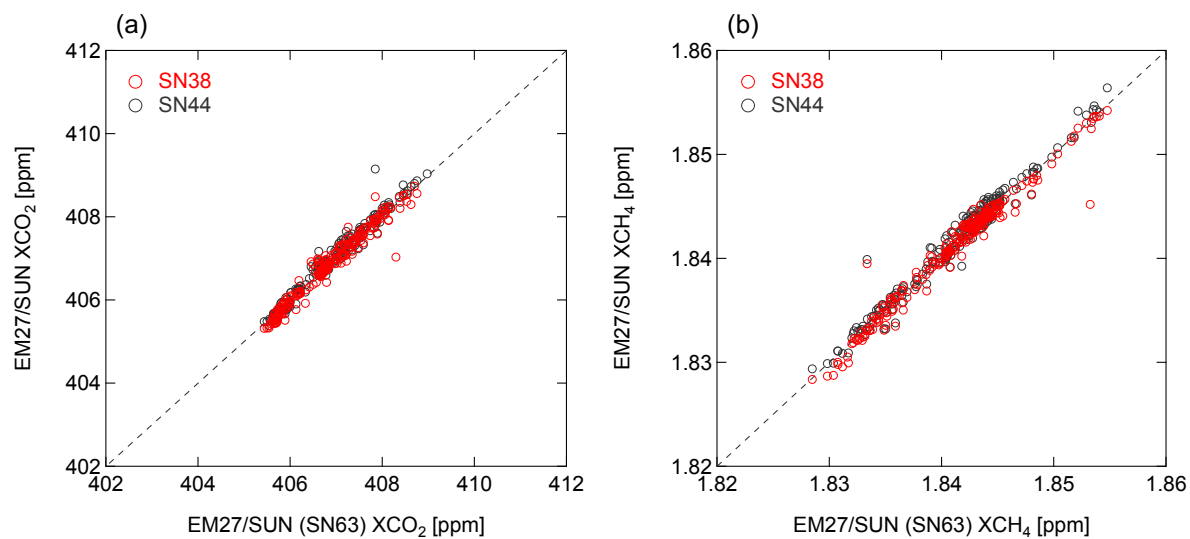


Figure S1. Scatter plots of bias-corrected SN38 and SN44 EM27/SUN data with respect to the SN63 EM27/SUN data for (a) XCO_2 and (b) XCH_4 . Dashed lines denote the one-to-one line.

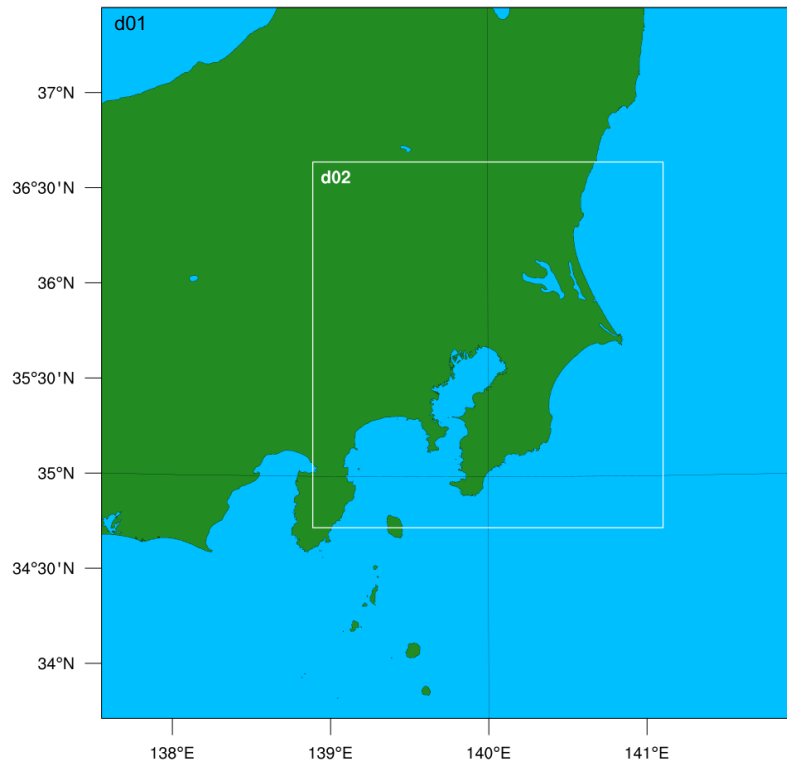


Figure S2. Domain configuration for the WRF simulation.

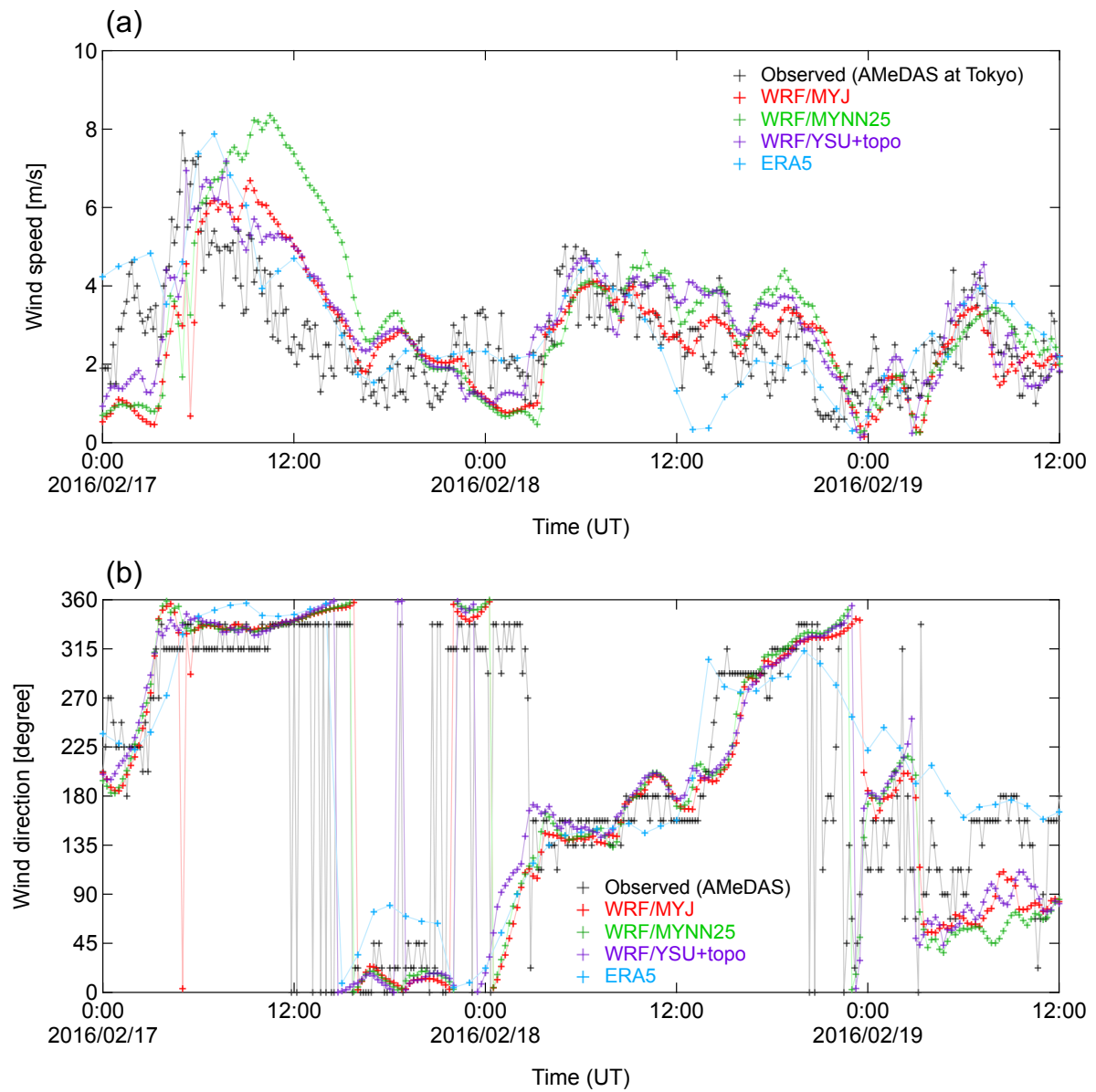


Figure S3. (a) Wind speed and (b) wind direction at the Tokyo AMeDAS station. The model data from the WRF simulations using different PBL schemes and the ERA5 reanalysis are also shown.

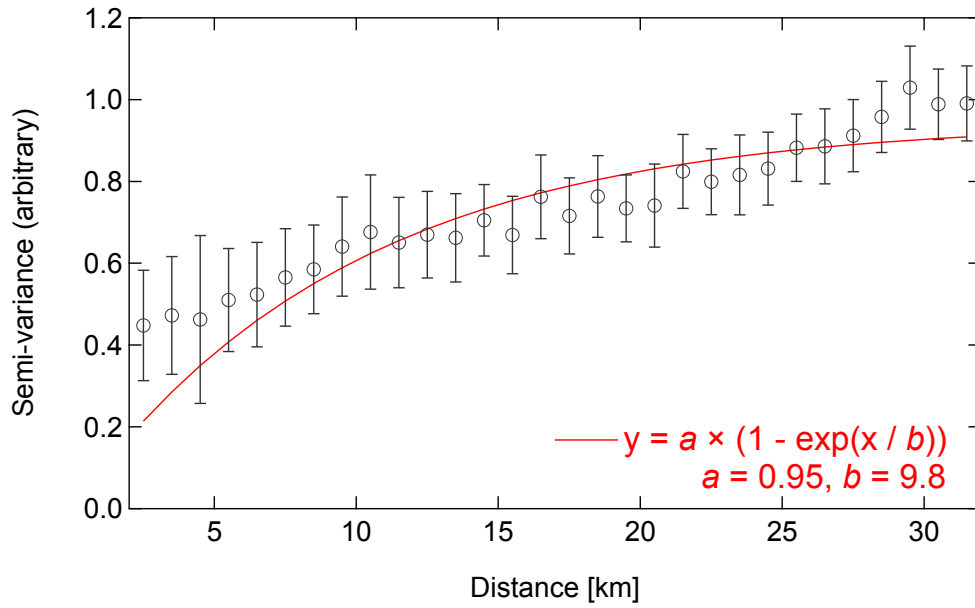


Figure S4. Semi-variogram calculated from the differences in nonpoint source elements between the ODIAC and MOSAIC emission data with both aggregated into a spatial resolution of $0.025^\circ \times 0.025^\circ$. The error bars indicate the standard error of each 1 km bin. The red line is the fitted curve with coefficients a and b , where coefficient b corresponds to the spatial correlation length.

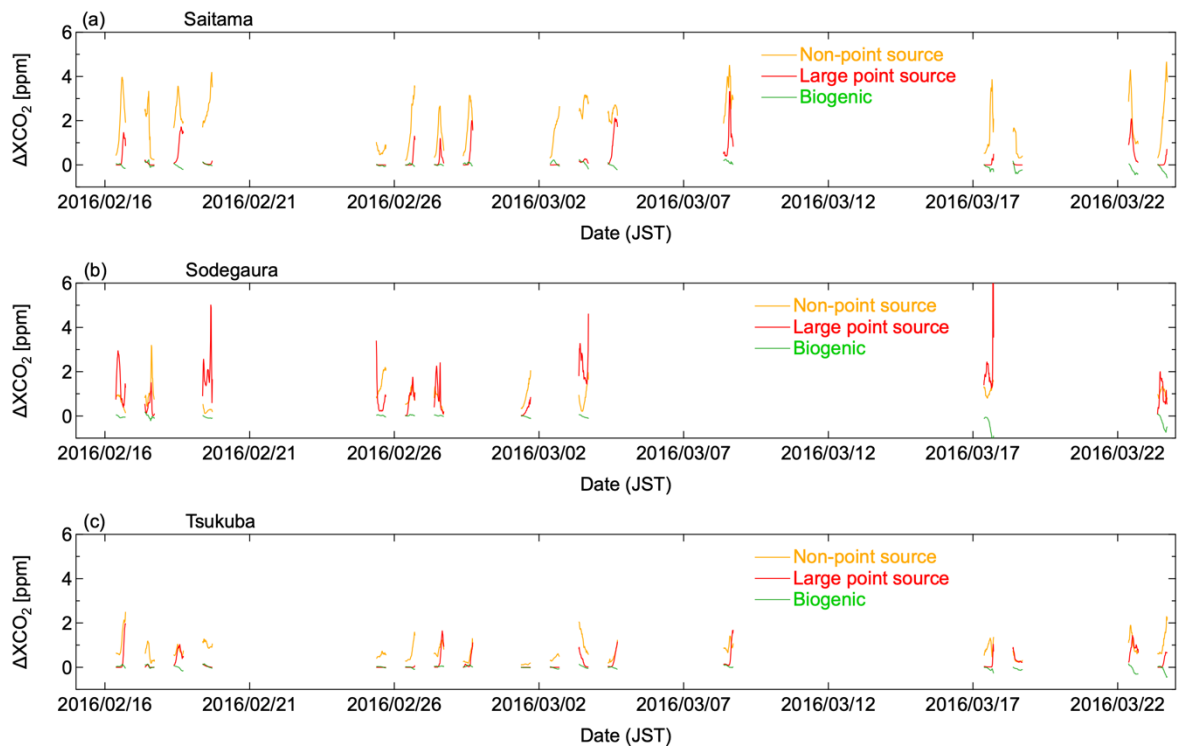


Figure S5. ΔXCO_2 values at (a) Saitama, (b) Sodegaura, and (c) Tsukuba simulated separately from nonpoint sources, large point sources, and biogenic fluxes.

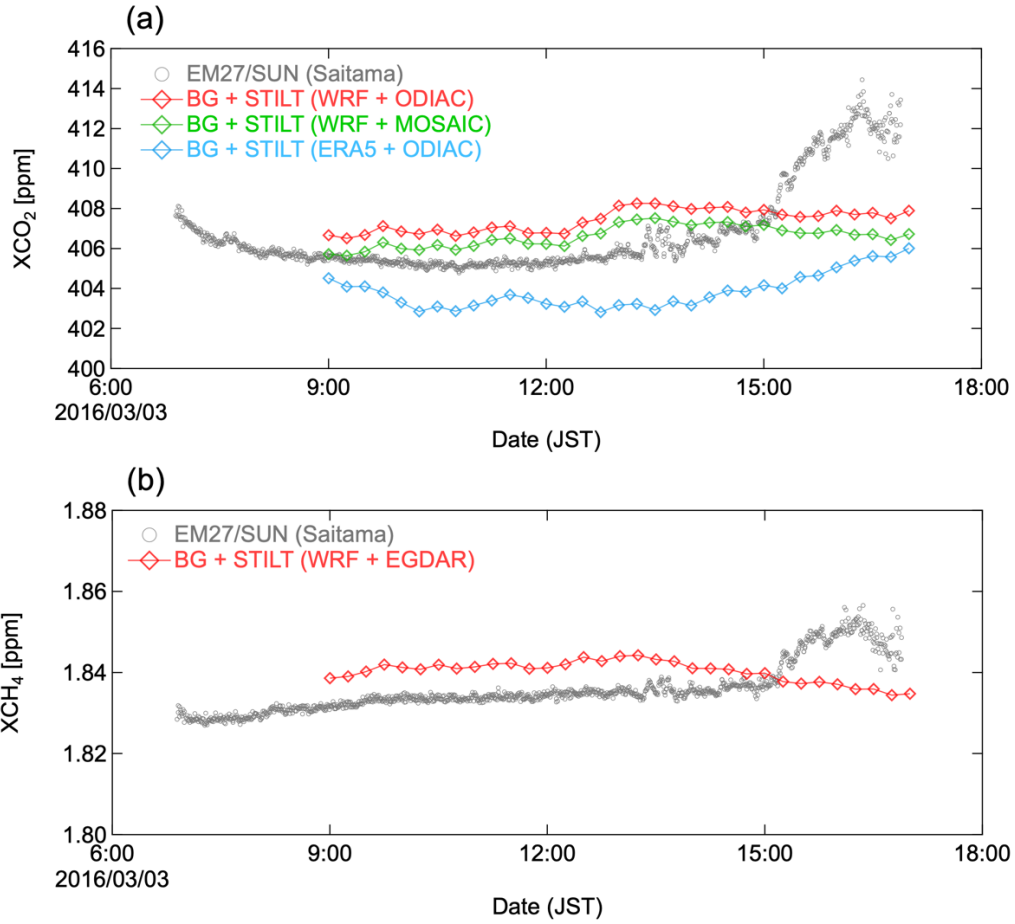


Figure S6. Comparison of (a) XCO₂ and (b) XCH₄ observations at Saitama on 3 March 2016 with STILT simulation results. The XCO₂ simulations were performed using three different combinations of meteorological fields and emission data, whereas the XCH₄ simulation was performed using the WRF model and EDGAR data.

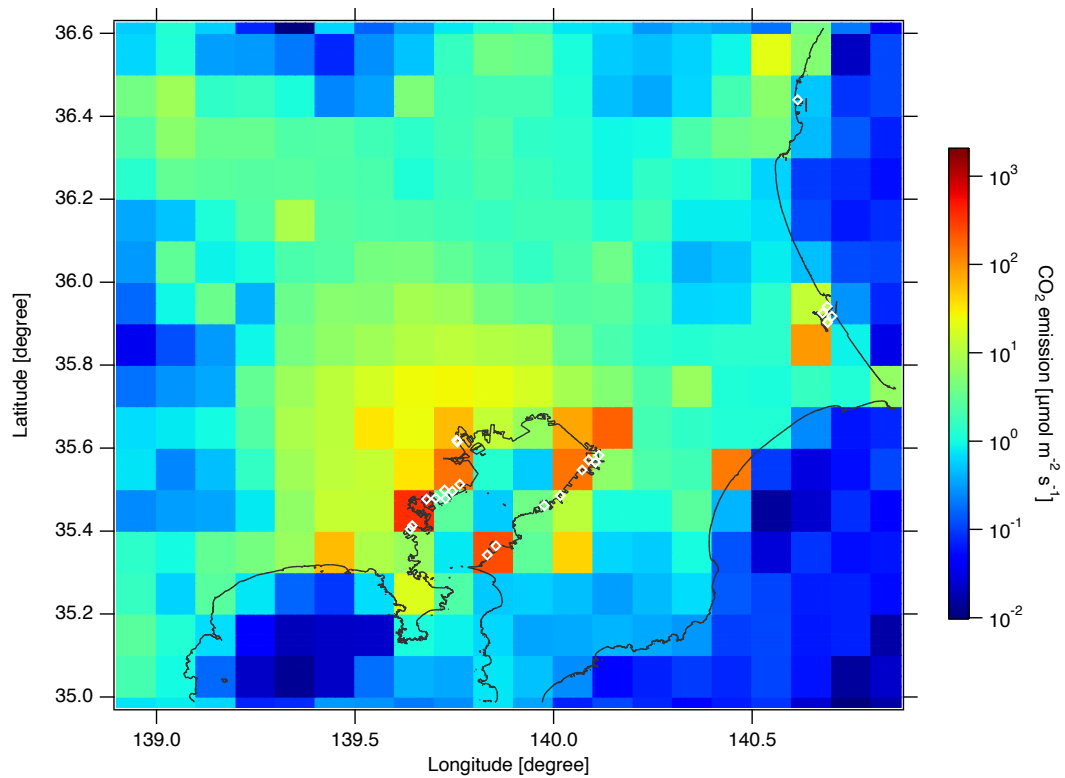


Figure S7. EDGAR version 6 CO₂ emission fluxes in the TMA in 2016. White diamonds indicate the locations of the large point sources considered in this study.

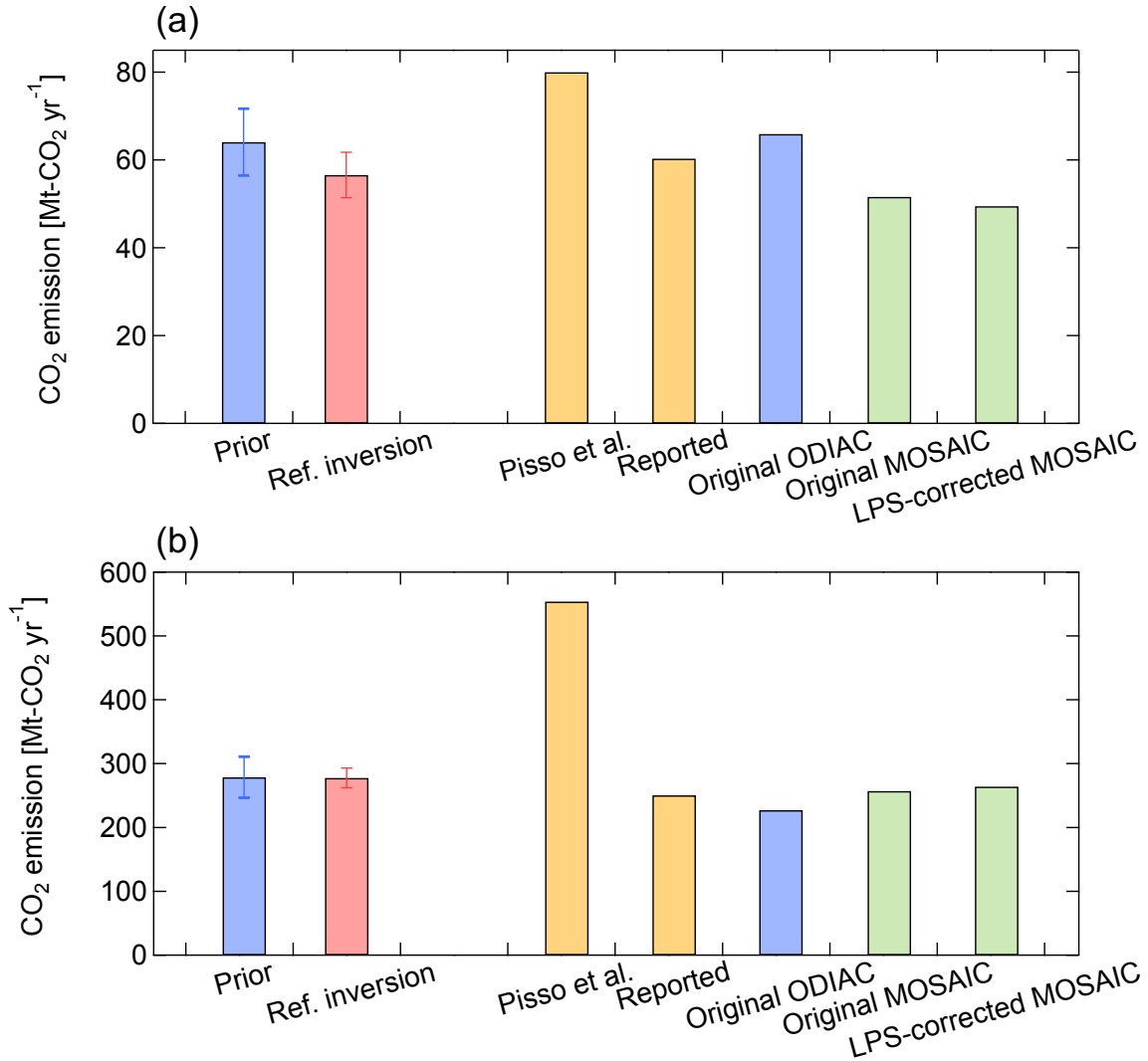


Figure S8. CO₂ emissions in (a) the Tokyo Metropolis and (b) southern Kanto (Tokyo Metropolis and Kanagawa, Saitama, and Chiba Prefectures) calculated from the posterior fluxes of the reference inversion (red), the ODIAC data (blue), and the MOSAIC data (green). The error bars for the prior and posterior estimates indicate uncertainties at the 95 % confidence level. For the ODIAC and MOSAIC data, both original and LPS-corrected total emissions are shown. Also shown are the CO₂ emissions for the corresponding domains extracted from Pisso et al. (2019) and the values reported by the administrative divisions (yellow).